Chemical Physics 588 (2025) 112464

Contents lists available at ScienceDirect

Chemical Physics

journal homepage: www.elsevier.com/locate/chemphys

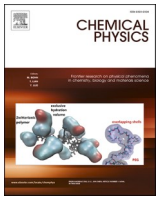

A study using physical sphere-in-contact models to investigate the structure of close-packed nanoparticles supported on flat hexagonal, square and trigonal lattices

Constantinos D. Zeinalipour-Yazdi [a,b]

[a] Faculty of Computing, Mathematics, Engineering and Natural Sciences, Northeastern University London, E1W 1LP, UK
[b] Department of Mechanical and Aerospaces, Brunel University London, Uxbridge UB8 3PH, UK

ARTICLE INFO

Keywords:
Sphere-in-contact
NPs
Nanoparticles
Metal Surface
Close-packed

ABSTRACT

The tailored design of nanoparticles becomes more important with the advancement of heterogeneous catalysis and materials science. The formation of nanoparticles in catalysts with a specific geometry of the active site becomes necessary to improve activity and selectivity in catalysis. Here we have used physical sphere-in-contact models of various nanoparticles with hexagonal, square and trigonal geometries on flat close-packed surfaces to understand how the distribution of (100) and (111) sites changes as a function of nanoparticle (NP) size in a simplified model of nanoparticle supported metals. The results from this approach clearly show that in 2-layer NPs that have a hexagonal base have 2–3 times more (100) sites than the square and trigonal base NPs as a function of the number of atoms in the NP. In 3D isotropic NPs, this phenomenon is even more pronounced than the 2-layer NPs. We derive equations that estimate the number of (100), (111), the number of atoms and the aspect ratio as a function of n. These equations are important in tailoring the properties of NPs supported on close-packed metal surfaces, which may find applications in materials science, nanotechnology and catalysis.

1. Introduction

The use of physical molecular models in research is becoming important due to the possibility to print molecular models with a 3D printer [1,2]. These models have been mainly used as an educational tool to understand the structure and property of molecules, materials and biomolecules. In particular, they have been used to teach VSEPR theory [3], symmetry [4,5], orbital theory [6,7] electron density iso-surfaces [8] and the operation of diffraction gratings [9]. However, physical molecular models can also been used in research and to discover new properties of matter and biomolecules. For example, Watson and Crick have used physical molecular models of DNA to understand the H-bonding and the structure of base pairs [10]. Sir William Bragg used physical molecular models to understand the structure of crystals [11]. We have previously used the sphere-in-contact model to build molecular models of carbon materials [12,13] that had scale and the right proportions. Furthermore, we have used the sphere-in-contact models to elucidate the cap structure in (3,3)-SWCNT, (4,4)-SWCNT and (5,5)-SWCNT [14,15]. The sphere-in-contact model was also used to find a X-Ray filter that was based on the structure of rhombohedral graphite [16]. We have also used magnetic ball-and-stick models to understand the topology of the active site in HCP and FCC metal nanoparticles and surfaces [17]. This study showed clearly that physical molecular models can be handled in ways that are beyond the capability of computer programes used in molecular modeling. The main advantage being that, with the physical molecular models, you can discover in a visual and practical way, whereas in computer programs the discovery relies entirely on the visual component. Furthermore these models may become education tools in surface science and catalysis as they can depict and manipulate the structure of supported metal NPs.

The structure of metal NPs supported on surfaces is of fundamental importance in materials science and catalysis. Investigating the size dependence of NPs is essential as it plays a critical role in determining their physical and chemical properties, which have significant implications in various fields [18,19]. Understanding the topology of the active site in catalysis is essential for the modeling of reaction mechanisms. Metal nanoparticles that have HCP or FCC structures are known to have (100) and (111) sites on their surfaces. These sites may generally undergo different catalytic reaction mechanisms and therefore it is important to investigate their distribution as a function of NP size on surfaces. In this investigation we have used physical sphere-in-contact models to study the structure and topology of various 2-layer and 3D

E-mail addresses: constantinos.zeinalipour@nulondon.ac.uk, zeinalip@gmail.com.

https://doi.org/10.1016/j.chemphys.2024.112464
Received 15 March 2024; Received in revised form 24 July 2024; Accepted 18 September 2024
Available online 22 September 2024

isotropic metal nanoparticles on flat hexagonal, square and trigonal surfaces. The study reveals that the number of (100) and (111) sites (see scheme 1) on the metal nanoparticle can be given by mathematical equations that correlate these properties to the number of atoms in the NP. Furthermore, the number of atoms in the NP and the aspect ratio can be expressed as a function of a dimensionless parameter, n.

In scheme 1 you can see that in the sphere-in-contact model the atoms have their corresponding atomic radius and the spheres are just touching at a point that binds the two atoms. This model has been previously used succesfully to provide realistic models of carbon materials (e.g. fullerene, graphene, graphite, carbon nanocones) [12], to elucidate the cap structure of carbon nanotubes [15] and how radiation interacts with the channels in rhombohedral graphite [16].

The rest of this paper has the following structure. First we present for n = 1–6 the 2-layer NP on hexagonal, square and trigonal grids. For these, we plot the number (111) and (100) sites and the aspect ratio as a function of n. We then present 3D hexagonal, square and trigonal NPs on a close-packed surface for which we plot the number of (111) and (100) sites as a function of the number of metal atoms in the NP. Various mathematical derivations are given in the Appendix.

2. Results and Discussion

Modeling the growth of NP on surfaces is possible with the sphere-in-contact model in a simplified process although it does not encompass structures that diverge from strict close-packed packing such as icosahedral and decahedral motifs. We have considered both 2-layer NPs that are either symmetric or assymmetric and 3D NP, that are more than two layers high. The NPs were built on a hexagonal and square grid and therefore the base of the NP was either hexagonal (see Fig. 1b), square (see Fig. 1c) or trigonal (see Fig. 1a). When building these geometries, we only consider NP in which each layer is smaller than the previous base layer. For these NPs we derive equations that can predict the number of atoms in the NP, the aspect ratio and the number of (100) and (111) sites.

2.1. 2-layer asymmetric hexagonal, square and trigonal NPs on close-packed lattices of metals

The stacking of the spheres in these models is AB. We only studied the NP growth when this happened in 1 direction. The shape of the NP is described by the aspect ratio, which is defined as the long dimension (a) divided by the short dimension of the NP (b). Being able to define the shape of NP is critical in nanotechnology as such shapes may be components of novel materials with new properties different than the bulk materials.

In Fig. 1 we present for n = 1 to n = 6 the sphere-in-contact model of NPs that has a trigonal base, a hexagonal base and a square base.

In Table 1 we present the number of atoms, the number of (100) sites, the number of (111) sites and the aspect ratio (a/b) for the various 2-layer NPs. The last row of this table provides the mathematical formula as a function of n that can calculate the various parameters in the NP. Equations of this type are particularly important for the controlled design of catalytic materials. For example the number of (100) sites versus the (111) sites can give us a quantitative measurement of the number of catalytic centers that have different geometries and therefore will undergo different mechanisms in catalytic reactions. This has significant implications in catalysis and in understanding the pathway of catalytic reactions on nanoparticles. Furthermore, the aspect ratio of the NP is an important parameter in the design of new materials. The derivation of clear mathematical equation can therefore have significant implications of modelling catalysts and catalytic reaction mechanisms.

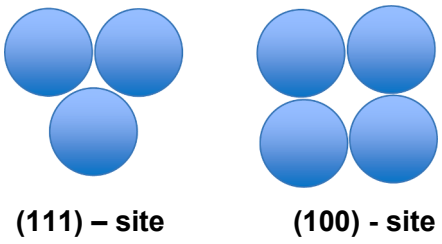

Scheme 1. Sphere-in-contact model of (111) and (100) sites on metal nanoparticles.

The number of atoms in the hexagonal base NP is 5(n + 1). The number of (100) sites changes as n + 2 in the hexagonal base NPs. This is much lower than the number of (111) sites that changed as 4n. The aspect ratio is given by (n + 2)/(1+$\sqrt{3}$). These simple equations describing the NP may become important in the mathematical modeling of NPs for technological applications.

In Fig. 2 we present the correlation between (100) sites and the number of atoms in the NP. One can clearly see that the number of (100) sites in hexagonal NPs exceeds that of the square base and triangular base NP. This property might find application in catalysis and nanotechnology, as (100) sites have different catalytic properties of (111) sites in metal NPs [20,21]. Furthermore the magnetic properties of (100) sites will be different than the magnetic properties of (111) sites. This has previously been observed in Co adatoms and monolayers deposited on various Miller index surfaces (e.g. (100), (111) and (110)) where changes in the crystallographic orientation has a large effect on the orbital magnetic moment and a dramatic effect on the magnetocrystalline anisotropy energy and on the magnetic dipole term T [22]. Furthermore the magnetic moments of metal monolayers on closed-packed surfaces are known to drastically change the magnetic moment of the atoms at the surface compared to atoms in the bulk [22,23]. Lastly, the type of surface sites (i.e. (111) or (100)) also affect the coverage-dependent adsorption energy of adsorbates [21,24]. It is therefore evident that knowledge of the relative numbers of (100) and (111) sites in NP is critical in the design of more selective catalysts and nanomaterials with tailored properties.

The number of atoms, number of (111) and (100) sites as a function of n and the aspect ratio of square base NPs is given in Table 2. The number of atoms in the square base NP is 8 + 5n. The number of (100) sites changes as n in the square base NPs. This is much lower than the number of (111) sites that changed as 4(2 + n). The aspect ratio is given by (n + 2)/3. This suggests that the aspect ratio of square base NPs is slightly larger than that of hexagonal base NP.

Fig. 3 shows a graph of the number of (111) sites and a function of the number of atoms in the NPs. We observe that trigonal base NPs have more (111) sites, followed closely by square base NPs and the lowest number of (111) sites is observed in the hexagonal base NPs. This is a very useful result as it predicts that NP grown trigonally on (111) metal surfaces will also have more (111) sites on their surface.

The number of atoms, number of (111) and (100) sites as a function of n and the aspect ratio of trigonal base NPs are given in Table 3. The number of atoms in the trigonal base NPs is 4 + 5n. The number of (100) sites changes as n-1 in the square base NPs. This is much lower than the number of (111) sites that changed to 2(3 + 2n). The aspect ratio is given by (n + 2)/(1+$\sqrt{3}$). This suggests that the aspect ratio of trigonal base NPs is almost the same as that of hexagonal base NPs, which is in agreement with the fact that the NPs were grown on the same lattice (i.e. hexagonal).

In Fig. 4 we graph the aspect ratio of the various 2-layer NPs on hexagonal, trigonal and square lattices. We find that for 2-layer NPs the aspect ratio of trigonal base NPs is the greatest, followed closely by hexagonal base NPs. The aspect ratio of square base NPs is much lower than that of hexagonal and trigonal. This is important when synthesising NP on metal surfaces that have properties that depend on their aspect ratio. It is also important in the use of metal NP as pharmaceutical agents as the aspect ratio will determine the penetration depth of these NPs in solid tissue [25].

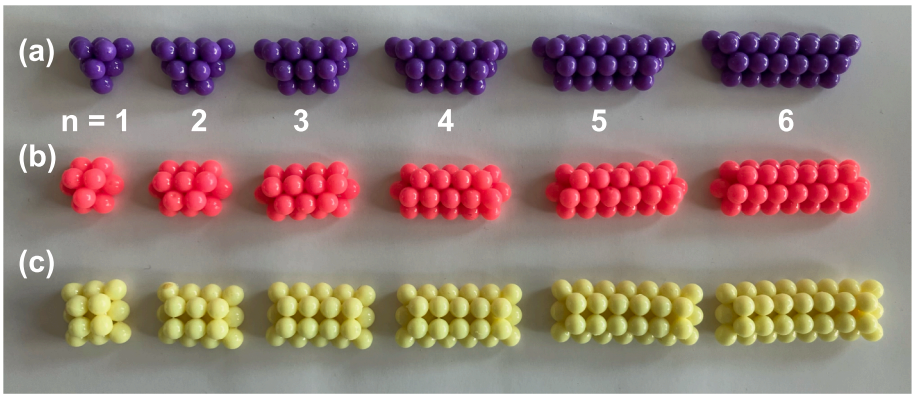

Fig. 1. Sphere-in-contact models of asymmetric (a) trigonal, (b) hexagonal and (c) square NPs supported on lattices supported on close-packed surfaces of metals.

Table 1
Asymmetric 2-layer hexagonal nps supported on flat close-packed surface.

n	# of atoms	#(100) sites	#(111) sites	aspect ratio (a/b)
1	10	3	4	1.10
2	15	4	8	1.46
3	20	5	12	1.83
4	25	6	16	2.20
5	30	7	20	2.56
6	35	8	24	2.93
n	5(n + 1)	n + 2	4*n*	(n + 2)/(1+√3)

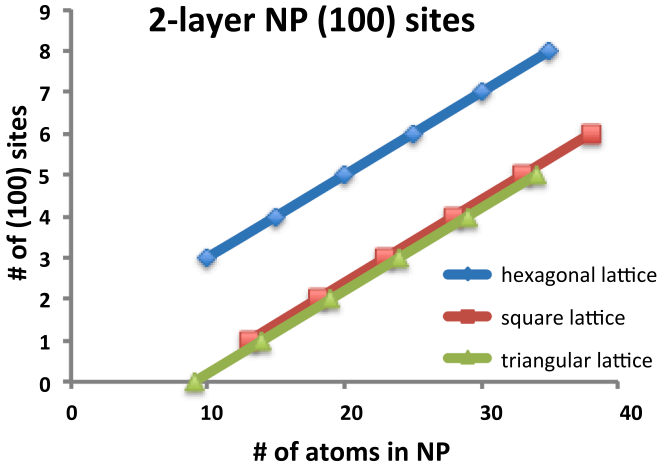

Fig. 2. Graph of the number of (100) sites on the 2-layer NP surface in hexagonal, trigonal and square base NPs. The parameter n is a positive integer that obtains values from 1, 2, 3, 4, …, n. As n increases so does the mass, dimension and the number of metal atoms in the NP increase.

Table 2
Asymmetric 2-layer square NPs supported on flat close-packed surface.

n	# of atoms	#(100) sites	#(111) sites	aspect ratio (a/b)
1	13	1	12	1.00
2	18	2	16	1.33
3	23	3	20	1.67
4	28	4	24	2.00
5	33	5	28	2.33
6	38	6	32	2.67
n	8 + 5*n*	n	4(2 + n)	(n + 2)/3

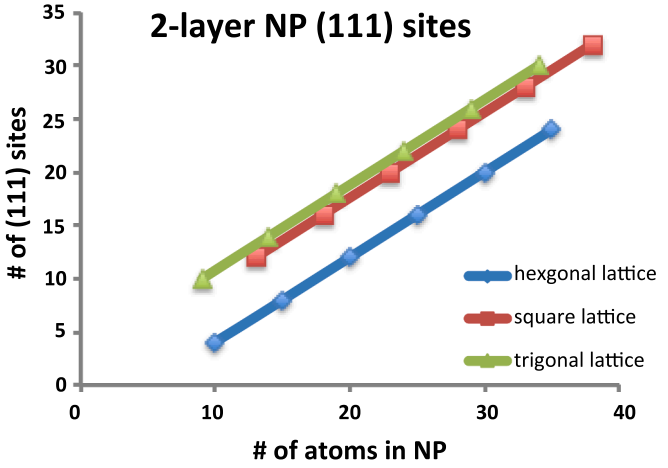

Fig. 3. Graph of the number of (111) sites on the 2-layer NP surface in hexagonal, trigonal and square base NPs.

Table 3
Asymmetric 2-layer trigonal nps supported on flat close-packed surface.

n	# of atoms	#(100) sites	#(111) sites	aspect ratio (a/b)
1	9	0	10	1.10
2	14	1	14	1.46
3	19	2	18	1.83
4	24	3	22	2.20
5	29	4	26	2.56
6	34	5	30	2.93
n	4 + 5*n*	n-1	2(3 + 2n)	(n + 2)/(1+√3)

2.2. 3D hexagonal, square and trigonal NPs on close-packed surface

In Fig. 5 we present various sphere-in-contact models of NPs that are deposited on trigonal (Fig. 5a), square (Fig. 5b) and hexagonal (Fig. 5c) lattices. The NPs that have a trigonal base protrude the most, followed by the NPs that have a square base, followed by the NPs that have a hexagonal base. The trigonal and square base NPs only expose (1 1 1) surfaces, whereas the hexagonal base NPs expose both (1 1 1) and (1 0 0) facets in roughly equal numbers. It is therefore evident that the selectivity of catalytic reactions will be enhanced on the trigonal and square base NPs, whereas the hexagonal base NPs will potentially exhibit two reaction mechanistic pathways at least, corresponding to the (1 0 0) and (1 1 1) facets of the NP.

The arrangement of the atoms in these NP resembles the arrangement of cannonballs on ships in the 15th century when Thomas Harriot was given this problem to solve by Sir Walter Raleigh on their journey to

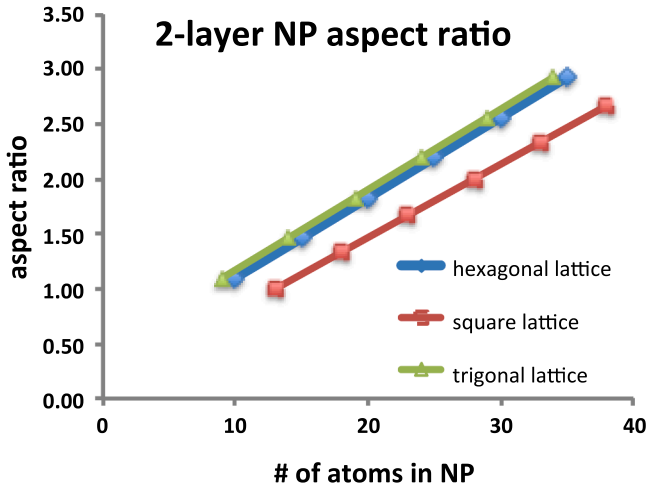

Fig. 4. Graph of the aspect ratio of 2-layer NPs hexagonal, trigonal and square lattices as a function of the number of atoms in the NP.

America [26]. In these close-packed models, the NP with the square base and the triangular base form FCC lattices whereas the ones with the hexagonal base form HCP lattices.

In Table 4 we present the number of atoms, the number of (100) sites and the number of (111) in isotropic hexagonal base NPs. We mathematically derive the number of atoms in these NPs, which is given by,

$$\Sigma_1 = \sum_{n=1}^{k+1} n + \sum_{n=1}^{k+3} n + \cdots + \sum_{n=1}^{3k+1} n - 3\left(\sum_{n=1}^{1} n + \sum_{n=1}^{2} n + \sum_{n=1}^{3} n + \cdots + \sum_{n=1}^{k} n\right) \quad (1)$$

The number of atoms increases drastically in these NP as a function of n.

In Table 5 we present the number of atoms, the number of (100) sites and the number of (111) sites as a function of n in square base NPs.

The total number of atoms in the square base NPs was previously derived by the French mathematician François Édouard Anatole Lucas who formulated the problem as the Diophantine equation given by,

$$\Sigma_2 = \sum_{n=1}^{N} n^2 = M^2 \quad (2)$$

The number of (100) sites is zero and the number of (111) sites is $4(1 + n)^2$.

In Table 6 we present the number of atoms, the number of (100) sites and the number of (111) sites as a function of n in trigonal base NPs. Here the number of (100) sites is 0 and the number of (111) sites goes as $3(n + 2)^2$. The equation that yields the total number of atoms in the NP is given by,

$$\Sigma_3 = \sum_{n=1}^{k+3} n! \quad (3)$$

In Fig. 6 we graph the number of (111) sites (see Fig. 6a) and the number of (100) sites (see Fig. 6b) as a function of the number of metal atoms in the NP. The results show that NP with a trigonal base has the highest number of (111) sites followed closely by NP with a square base. Whereas the NP with a hexagonal base has the lowest number of (111)

Table 4
Isotropic hexagonal NP supported on flat close-packed surface.

n	# of atoms	#(100) sites	#(111) sites
1	10	3	4
2	37	12	16
3	92	27	36
n	Σ_1	$3n^2$	$(2n)^2$

Table 5
Isotropic square NP supported on flat close-packed surface.

n	# of atoms	#(100) sites	#(111) sites
1	15	0	16
2	30	0	36
3	55	0	64
4	91	0	100
n	*	0	$4(1 + n)^2$

* # of atoms was found by measuring the atoms in the NP model (5b).

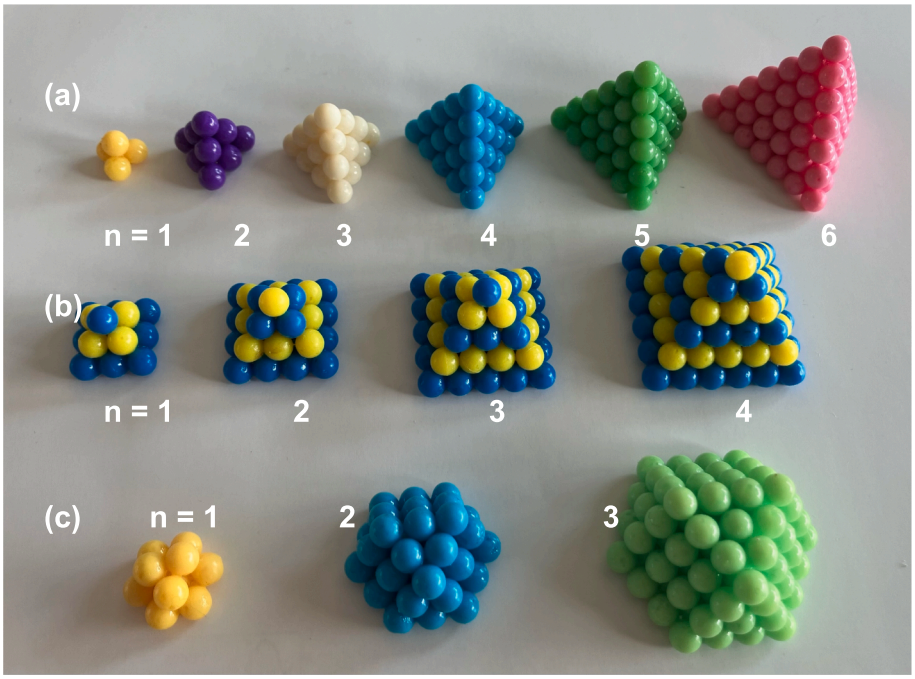

Fig. 5. Sphere-in-contact models of closed-packed isotropic (a) trigonal, (b) square and (c) hexagonal NPs supported on close-packed surfaces.

Table 6
Isotropic trigonal NP supported on flat close-packed surface.

n	# of atoms	#(100) sites	#(111) sites
1	20	0	27
2	35	0	48
3	56	0	75
4	84	0	108
n	Σ_3	0	$3(n+2)^2$

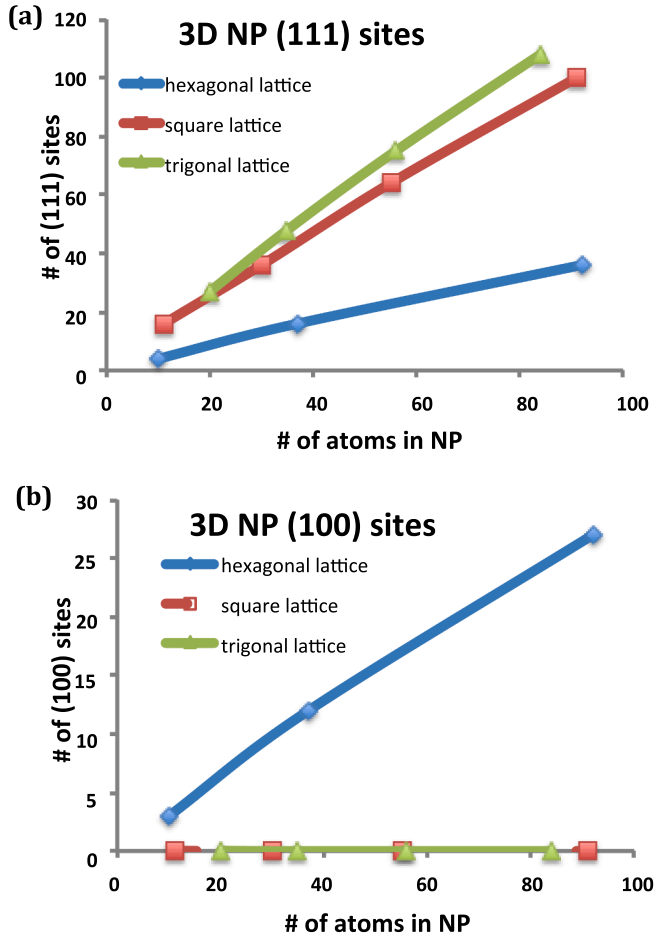

Fig. 6. Graph of the number of (a) (111) sites and (b) (100) sites 3D isotropic NPs on hexagonal, trigonal and square lattices as a function of the number of atoms in the NP.

sites. The equations that can calculate the number of (111) and (100) sites in these 3D isotropic NPs are,

$$\text{Trigonal base NPs}, n_{111} = 1.3110\ N \quad (4)$$

$$\text{Square base NPs}, \ n_{111} = 1.1257\ N \quad (5)$$

$$\text{Hexagonal base NPs}, n_{111} = 0.3971\ N \quad (6)$$

$$\text{Trigonal base NPs}, \ n_{100} = 0N \quad (7)$$

$$\text{Square base NPs}, n_{100} = 0\ N \quad (8)$$

$$\text{Hexagonal base NPs}, n_{100} = 0.2978\ N \quad (9)$$

, where N is the number of metal atoms in the NP and n_{111}/n_{100} the number of (111) and (100) sites on the surface of the NP, respectively.

3. Conclusions

In conclusion, the sphere-in-contact model has proven to be a simple yet useful tool for understanding the structure of nanoparticles on flat hexagonal, cubic, and trigonal lattices. Its application has allowed us to analyze the packing arrangements, explore crystal growth processes, and predict the surface characteristics of nanoparticles within these lattice systems as a function of (1 1 1) and (1 0 0) sites on the surface of the NP. We derive analytical equations that can predict the number of (1 1 1) and (1 0 0) sites on the surface of a NP and the number of atoms in the NP supported on hexagonal and square lattices. Equations are also provided that can predict the aspect ratio of NP that grow on different substrates as a function of NP size. The knowledge gained from these investigations can contribute to the rational design and engineering of nanoparticle-based materials with tailored properties and functionalities. Finally, it can assist scientists that do single crystal studies of heterogeneous catalysts to address questions concerning the structure–reactivity of supported metal nanoparticles on (1 1 1) surfaces of metals. We anticipate that this study maybe used as a model for the controlled design of nanoparticles deposited on surfaces.

4. Declarations

Availability of data and material: The datasets generated during and/or analysed during the current study are available from the author on reasonable request.

Authors' contributions: This study was conceived, designed by Dr. Constantinos Zeinalipour-Yazdi. CDZ did the analysis of the models and wrote the paper.

Funding

The author declares that no funds, grants, or other support were received during the preparation of this manuscript.

6. Author statement

1. The conception and design of the study, or acquisition of data, or analysis and interpretation of data was done by Dr. Constantinos Zeinalipour-Yazdi.
2. All graphs and interpretations were done by Dr. Constantinos Zeinalipour-Yazdi
3. The manuscript was written entirely by Dr. Constantinos Zeinalipour-Yazdi

CRediT authorship contribution statement

Constantinos D. Zeinalipour-Yazdi: Writing – original draft, Visualization, Methodology, Investigation, Formal analysis, Data curation, Conceptualization.

Declaration of competing interest

The authors declare that they have no known competing financial interests or personal relationships that could have appeared to influence the work reported in this paper.

Data availability

Data will be made available on request.

Acknowledgement

The authors would like to thank the Northeastern University Library for covering the APC charge to make this paper open access. The author also wishes to acknowledge Christos Koulas for helping in the derivation of Eqn. 1.

Appendix

$$\Sigma_1 = \sum_{n=1}^{k+1} n + \sum_{n=1}^{k+3} n + \cdots + \sum_{n=1}^{3k+1} n - 3\left(\sum_{n=1}^{1} n + \sum_{n=1}^{2} n + \sum_{n=1}^{3} n + \cdots + \sum_{n=1}^{k} n\right) \quad (1)$$

We have counted the atoms in in each layer of the NP and found the following relationships from which the mathematical equations were derived.

For the hexagonal grid:

For n = 1
$2 + 1\text{–}0 = 3$
$4 + 3 + 2 + 1\text{-}3x1 = 7$

For n = 2
$4 + 3 + 2 + 1\text{–}0 = 10$
$6 + 5 + 4 + 3 + 2 + 1\text{-}3x1 = 12$
$7 + 6 + 5 + 4 + 3 + 2 + 1\text{-}3x(2 + 1) = 19$

For n = 3
$4 + 3 + 2 + 1\text{–}0 = 10$
$6 + 5 + 4 + 3 + 2 + 1\text{-}3x1 = 18$
$8 + 7 + 6 + 5 + 4 + 3 + 2 + 1\text{-}3x(2 + 1) = 27$
$10 + 9 + 8 + 7 + 6 + 5 + 4 + 3 + 2 + 1\text{-}3x(3 + 2 + 1) = 37$

For the trigonal grid.

For n = 1
$4 + 3 + 2 + 1 = 10 \rightarrow 4!$
$3 + 2 + 1 = 6 \rightarrow 3!$
$2 + 1 = 3 \rightarrow 2!$
$1 = 1 \rightarrow 1!$

$$\Sigma_a = \sum_{n=1}^{4} n! \quad (2a)$$

For n = 2
$5 + 4 + 3 + 2 + 1 = 15 \rightarrow 5!$
$4 + 3 + 2 + 1 = 10 \rightarrow 4!$
$3 + 2 + 1 = 6 \rightarrow 3!$
$2 + 1 = 3 \rightarrow 2!$
$1 = 1 \rightarrow 1!$

$$\Sigma_b = \sum_{n=1}^{5} n! \quad (2b)$$

For n = 3
$6 + 5 + 4 + 3 + 2 + 1 = 21 \rightarrow 6!$
$5 + 4 + 3 + 2 + 1 = 15 \rightarrow 5!$
$4 + 3 + 2 + 1 = 10 \rightarrow 4!$
$3 + 2 + 1 = 6 \rightarrow 3!$
$2 + 1 = 3 \rightarrow 2!$
$1 = 1 \rightarrow 1!$

$$\Sigma_c = \sum_{n=1}^{6} n! \quad (2c)$$

for k = 1, 2, 3 … the equation becomes Eqn. 3

$$\Sigma_3 = \sum_{n=1}^{k+3} n! \quad (3)$$

References

[1] L.E.H. Violante, D.A. Nunez, S.M. Ryan, W.T. Grubbs, 3D printing in the chemistry curriculum: inspiring millennial students to be creative innovators. addressing the millennial student in undergraduate chemistry, ACS Symp. Ser. 1180 (2014) 125–146.

[2] O.A.H. Jones, M.J.S. Spencer, A simplified method for the 3d printing of molecular models for chemical education, J. Chem. Educ. 95 (2018) 88–96.

[3] N.L. Dean, C. Ewan, J.S. McIndoe, Applying hand-held 3d printing technology to the teaching of vsepr theory, J. Chem. Educ. 93 (2016) 1660–1662.

[4] L. Casas, E. Estop, Virtual and printed 3d models for teaching crystal symmetry and point groups, J. Chem. Educ. 92 (2015) 1338–1343.

[5] V.F. Scalfani, T.P. Vaid, 3D printed molecules and extended solid models for teaching symmetry and point groups, J. Chem. Educ. 91 (2014) 1174–1180.

[6] M.J. Robertson, W.L. Jorgensen, Illustrating concepts in physical organic chemistry with 3d printed orbitals, J. Chem. Educ. 92 (2015) 2113–2116.

[7] K.M. Griffith, R.d. Cataldo, K.H. Fogarty, Do-It-Yourself: 3D Models of Hydrogenic Orbitals through 3D Printing, J. Chem. Educ. 93 (2016) 1586−1590.

[8] M. Garcia, F.A. O'Leary, D.J. O'Leary, Do-It-yourself 5-Color 3D printing of molecular orbitals and electron density surfaces, J. Chem. Educ. 100 (2023) 1648–1658.

[9] P.A.E. Piunno, Teaching the operating principles of a diffraction grating using a 3d-printable demonstration kit, J. Chem. Educ. 94 (2017) 615–620.

[10] J. Watson, F. Crick, A structure for deoxyribose nucleic acid, Nature 171 (1953) 737–738.

[11] S.W. Bragg, Concerning the Nature of Things, G. Bell and Sons Ltd, Six Lectures delivered at the Royal Institution, 1925.

[12] C.D. Zeinalipour-Yazdi, D.P. Pullman, C.R.A. Catlow, The sphere-in-contact model of carbon materials, J. Mol. Model. 22 (2016) 40.

[13] C.D. Zeinalipour-Yazdi, Doctoral thesis presentation "Electronic Structure and Interlayer Binding of Graphite", DOI: 10.13140/RG.2.2.13745.56168, (January 2006).

[14] C.D. Zeinalipour-Yazdi, E.Z. Loizidou, Corrigendum to "Study of the cap structure of (3,3), (4,4) and (5,5)-SWCNTs: Application of the sphere-in-contact model" [Carbon 115 819–827], Carbon 146 (2019) (2017) 369–370.

[15] C.D.L. Zeinalipour-Yazdi, E. Z., Study of the cap structure of (3,3), (4,4) and (5,5)-SWCNTs: Application of the sphere-in-contact model, Carbon 115 (2017) 819-827.

[16] C.D. Zeinalipour-Yazdi, D.P. Pullman, Study of a rhombohedral graphite X-ray filter using the sphere-in-contact model, Chem. Phys. Lett. 734 (2019) 136717.

[17] C.D. Zeinalipour-Yazdi, Topology of active site geometries in HCP and FCC nanoparticles and surfaces, Chem. Phys. 559 (2022) 111532.

[18] H. Kurban, M. Kurban, M. Dalkilic, Density-functional tight binding approach for the structural analysis and electronic structure of copper hydride metallic nanoparticles, Mater. Today Commun. 21 (2019) 100648.

[19] M. Kurban, I. Muz, Size-dependent adsorption performance of ZnO nanoclusters for drug delivery applications, Struct. Chem. 34 (2023) 1061–1071.

[20] M. Wang, H. Liu, J. Ma, G. Lu, The activity enhancement of photocatalytic water splitting by F- pre-occupation on Pt(100) and Pt(111) co-catalyst facets, Appl Catal B 266 (2020) 118647.

[21] C.J. Zhang, P. Hu, CO Oxidation on Pd(100) and Pd(111): a comparative study of reaction pathways and reactivity at low and medium coverages, J. Am. Chem. Soc. 123 (2001) 1166–1172.

[22] O. Šipr, S. Bornemann, H. Ebert, S. Mankovsky, J. Vackář, J. Minár, Co monolayers and adatoms on Pd(100), Pd(111), and Pd(110): Anisotropy of magnetic properties, Phys. Rev. B 88 (2013) 064411.

[23] D.-S. Wang, A.J. Freeman, H. Krakauer, Surface magnetism of a Ni overlayer on a Cu(001) substrate, Phys. Rev. B 24 (1981) 1126–1129.

[24] C. Liu, L. Zhu, X. Wen, Y. Yang, Y.-W. Li, H. Jiao, Hydrogen adsorption on Ir(111), Ir(100) and Ir(110)—surface and coverage dependence, Surf. Sci. 692 (2020) 121514.

[25] R. Agarwal, P. Jurney, M. Raythatha, V. Singh, S.V. Sreenivasan, L. Shi, K. Roy, Effect of shape, size, and aspect ratio on nanoparticle penetration and distribution inside solid tissues using 3D spheroid models, Adv Healthc Mater. 4 (2015) 2269–2280.

[26] D. Darling, "Cannonball problem" [online] Daviddarling.info. Available at: http://www.daviddarling.info/encyclopedia/C/Cannonball Problem.html [Accessed 26 Mar. 2018]. The internet encyclopedia of science Darling, D. (2018). Cannonball Problem. (2018).